Supplementary Information, Data S1

Structural basis for the impact of phosphorylation on the activation of plant receptor-like kinase BAK1

Contents **Page**

Supplementary Experimental Procedures

Protein production and crystallization

Arabidopsis BAK1-CD (residues 259–583) was cloned into a modified pET-28b vector with a small ubiquitin-like modifier (SUMO) protein fused at the N-terminus after the addition of 6×His tag. The plasmid was transformed into the *Escherichia coli* strain BL21 (DE3), which were then cultured at 37 ºC in a lysogeny broth (LB) medium containing 100 mg/L kanamycin. After the OD_{600} value reached 0.8, the culture was cooled to 16 ºC and supplemented with 0.5 mM isopropyl-β-D-thiogalactopyranoside (IPTG). After overnight induction, the cells were harvested through centrifugation, and the pellets were resuspended in the lysis buffer [20 mM Tris-HCl (pH 8.0), 150 mM NaCl, 4 mM $MgCl_2$, and 1mM ATP] and homogenized at 4 ºC using an ultra-high-pressure cell disrupter (JNBIO, Guangzhou, China). The insoluble material was removed through centrifugation at 12,000 rpm. The fusion protein was first purified via nickel-nitriloacetic acid (Ni-NTA) affinity chromatography and eluted using a lysis buffer. Ulp1 protease was subsequently added, and the protein was incubated at 16 ºC for 12 h to remove the 6×His-SUMO tag. The protein was then further purified via passage through a Mono-Q ion-exchange column (GE Healthcare). The purified BAK1-CD was brought to a final concentration of 20 mg/mL and stored at -80 ºC.

Crystallization was performed at 18 ºC using the hanging-drop vapor-diffusion technique. Crystals were obtained by mixing 1 μL of the protein solution

with an equal volume of the reservoir solution and equilibrating against 500 μL of the reservoir solution. The crystals for apo BAK1-CD was obtained in the reservoir solution containing 21% polyethylene glycol (PEG) 3350, 200 mM sodium citrate, 50 mM ammonium sulfate, and 20 mM 4-(2-hydroxyethyl)-1-piperazineethanesulfonic acid (HEPES) (pH 7.5). Crystals with good diffraction quality grew to a final size of 50 μm × 50 μm × 200 μm within 3 d. The BAK1-CD crystals in complex with AMP–PNP were obtained in the same well solution and supplemented with 2 mM AMP–PNP. The crystallization buffer is sufficient for cryoprotection. Thus, the crystals were directly flash-cooled in liquid nitrogen and then transferred into a dry nitrogen stream at -180 ºC for X-ray data collection.

X-ray data collection, processing, and structure determination

Native data for apo BAK1-KD crystals were collected at a resolution of 2.6 Å at 100 K using a MAResearch M165 CCD detector on a beamline 1W2A at the Beijing Synchrotron Radiation Facility. The diffraction data for BAK1-CD complexed with AMP–PNP were further collected at a resolution of 2.2 Å at -180 ºC using an ADSC Q315 CCD detector on a beamline BL17U at the Shanghai Synchrotron Radiation Facility. All data were processed and scaled using the HKL2000 package[1]. The crystals belong to the C2 space group, which has the following cell parameters: a = 70.1 Å, b = 74.7 Å, c = 71.9 Å, $\alpha = \gamma = 90°$, and $\beta = 93.7°$. One BAK1-CD molecule is present in the asymmetric unit in either the apo or complex form with a Matthews coefficient of 2.4 $Å^3$/Da, which corresponds to a solvent content of 45%[2].

The PHASER program[3] was used to determine the correct solution via the molecular replacement method using the crystal structure of interleukin-1 receptor-associated kinase (IRAK)-4 (PDB code: 2NRY)[4] as the initial searching model. The density map and model were displayed using COOT[5], and the inconsistency between the models of the BAK1-CD molecule was manually built. The complex structure was solved through the molecular replacement (MR) method using the apo BAK1-CD structure as the searching model. Several rounds of simulated annealing, restrained energy minimization, and individual B-factor refinement were conducted using PHENIX[6]. The model geometry was verified using the PROCHECK[7] software. Solvent molecules were located at stereochemically reasonable peaks in the σA-weighted *Fo-Fc* difference electron density map. The final refinement statistics are summarized in Table S5. The structural figures were drawn using the PyMOL[8] software. The coordinates and structural factors have been deposited in PDB database under the accession code 3UIM.

In vitro phosphorylation, protein digestion, and phosphopeptide enrichment

For the autophosphorylation analysis, the recombinant BAK1-CD and its mutants were first treated with dithiothreitol (DTT, 5 mM, at 37 ºC for 1 h) and iodoacetamide (20 mM, for 30 min in the dark) to reduce and alkylate the cysteine residues, and then digested overnight with sequencing-grade trypsin (Promega) at an E:S ratio of 1:40. Beta-casein digest was spiked in the BAK1

tryptic digest as the internal standard for mass spectrometric (MS) quantitation. Phosphopeptides present in the tryptic digests were enriched with TiO_2 microcolumns according to the manufacturer's instructions. In brief, the protein digest was mixed with a loading buffer [25% lactic acid, 80% acetonitrile (ACN), and 0.3% trifluoric acid] and loaded into the conditioned TiO_2 microcolumn through repetitive pipetting and centrifugation (1000×*g*, 10 min). After washing the microcolumn with buffer B once and with buffer A twice, the bound phosphopeptides were first eluted with 50 µL elution buffer I (20 µL 28% ammonium hydroxide in 480 µL ddH_2O), followed by elution with 50 and 30 µL elution buffer II (500 mM NH_4OH/60% acetonitrile). Each elution was conducted under centrifugation at 1000×*g* for 5 min. The eluates were dried in a speed vacuum and reconstituted in 0.1% formic acid/H_2O for MS analysis.

For the transphosphorylation analysis, FLS2-CD was first incubated with BAK1-CD wild-type or mutants at a ratio of 10:1 (wt/wt) in the kinase buffer [20 mM Tris–HCl, pH 7.5, 10 mM $MgCl_2$, 5 mM ethylene glycol tetraacetic acid (EGTA), 100 mM NaCl, and 1 mM DTT] supplemented with 0.1 mM ATP at 30 ºC for 1 h with gentle shaking. After the reaction, the protein mixture was digested with trypsin, and the phosphopeptides were enriched in a manner similar to that described above.

Liquid Chromatography with tandem mass spectrometry (LC-MS/MS) analysis for the identification of protein phosphorylation

The peptide samples were first loaded onto a Waters Symmetry C18 trapping column (300 μm i.d. × 1 cm length) at a flow rate of 8 μL/min using a Waters NanoAcquity ultrahigh-performance liquid chromatography (UPLC) system. After desalting and preconcentration, the peptides were separated via in-line gradient elution onto a 100 μm i.d. × 10 cm column packed with 1.7 μm BEH C18 material (Waters, Milford, USA) at a flow rate of 400 nL/min using a linear gradient from 2% to 35% B over 30 min (A = 0.1% FA in H_2O, B = 0.1% FA in ACN). The Waters Synapt Q-IM-time-of-flight (ToF) G1 mass spectrometer was operated at high-definition MS^E mode (high- and low-collision energy switching every 1.0 s), and the data were processed using ProteinLynx Global Server (PLGS version 2.4; Waters) to reconstruct the MS/MS spectra by combining all masses with similar retention times. The MS/MS spectra were searched against an internal database, which consists of the sequences of wild-type and various BAK1-CD mutants, as well as FLS2-CD, using PLGS and the following parameters: peak width, 0.3 min; MS and MS/MS tolerance, automatic (usually below 20 ppm); trypsin missed cleavages, 1; fixed modification, carbamidomethylation; variable modifications, Met oxidation and phosphorylation of Ser, Thr, or Tyr; and false positive rate, 4%.

Phosphopeptide identification had to meet the following requirements: (1) peptide hits are identified with a confidence of > 95% and a score of >5; (2) the mass error of the peptide precursor is below 10 ppm; and (3) phosphorylation sites are consistently assigned in at least three experimental replicates. In several cases, the MS/MS spectra were manually inspected to determine the

neutral loses and other spectral fragmentation features that are consistent with the putative modification sites.

Label-free quantitation of the relative changes in phosphorylation at specific sites

After the identification of the phosphopeptides and the assignment of the modification sites of BAK1 and FLS2, the quantitative response of each phosphopeptide was measured using the peak area of its extracted ion chromatogram (XIC) based on the accurate mass of the peptide precursor at a tolerance of 0.02 Da. Peptide ion extraction and peak area calculation were performed using the MassLynx software (Waters). The phosphopeptide derived from beta-casein (at 1031.415 *m*/*z*) was used as the internal standard to normalize the XIC peak response of the other phosphopeptides in the sample. The normalized XIC responses of the specific phosphopeptides (with known modification sites) in the BAK1 mutants were compared with those of their wild-type BAK1 counterparts to calculate the change percentages. For any phosphopeptide whose mass is expected to change through a point mutation, the theoretical mass of the peptide containing the mutated residue was calculated to obtain the XIC signals.

This quantitative workflow, which integrates phosphopeptide enrichment and LC-MS/MS, offers sufficient accuracy, reproducibility, and dynamic range for large-scale quantitative phosphoproteomics. We further verified the

reproducibility of the site-specific phosphorylation levels of wild-type BAK1 obtained from five replicates using this approach (Table S2).

Supplementary Information

Comparative analysis of the phosphorylation sites identified in different results

Previous studies by Clouse[9] and Nam[10] investigated the effect of BAK1 phosphorylation site mutations on the kinase function using classical biochemical approaches. Both autoradiography and anti-pThr blotting showed that the T455A mutant lost most of its autophosphorylation activity, whereas anti-pThr blotting indicated that the mutants of the other three pThr residues, namely, T446, T449, and T450, showed similar results, although to a lesser extent[9]. The autoradiography data may not reflect the accurate change in the overall phosphorylation levels, especially “the low level of autophosphorylation seen in T446, T449, T450 mutants allowed for greater uptake of phosphate from ^{32}P-ATP,” which would result in seemingly stronger radioactive signals by certain mutants other than the wild-type. In another assay that monitored the BRI1 phosphorylation of a peptide substrate as a functional readout of the BAK1 kinase activity, substitutions at T446 and T450 did not result in any loss in BAK1 activity compared with the wild type, whereas the activity of T449A was slightly lower. In a similar manner, single changes in T446, T449, and T50 on BAK1 did not affect its phosphorylation activity against BRI1 in yeast, whereas T455 was essential for its transphosphorylation activity.[10] By contrast, our results show that pT450 and pT455 were essential residues for both the auto- and transphosphorylation activities of BAK1 *in vitro*, whereas the effect of pT446 and pT449 was subtler. The discrepancy in the importance of pT450 shown in

previous studies and the present work is probably due to the different substrates used. BRI1, which is the receptor that detects BR signals, was the direct substrate of BAK1 in the previous assays[9, 10], whereas in the present study, FLS2, which detects the stimulation by a bacterial flagellin peptide (flg22), was the substrate used to measure the BAK1 transphophorylation activity. Our finding is in accordance with the *in vivo* data, suggesting that T450 is required in flg22-mediated growth repression uncoupled from BR signaling, as opposed to T446 and T449[9]. Considering that BAK1 participates in multiple pathways as a co-receptor, we speculate that specific phosphorylated residues of BAK1 may have differential significance on substrate phosphorylation and signal transduction[11]. These “regulatory” sites may be differentially phosphorylated *in vivo* by different ligand-triggered RLKs to activate distinct signaling pathways.

Supplementary Figures and Tables

Figure S1. Annotated sequence of BAK1-CD. The color scheme is consistent with the overall ribbon diagram shown in Figure 1B, i.e., light blue, N-lobe; orange, P-loop; pale green, C-lobe; yellow, catalytic loop; and red, activation loop.

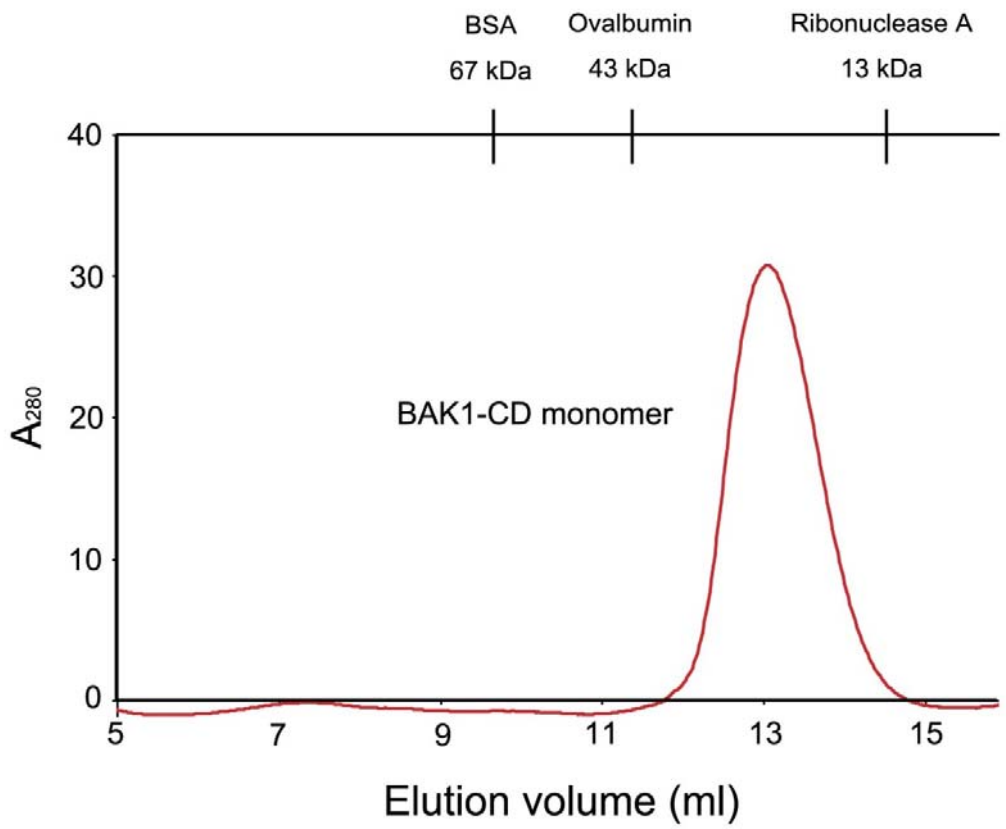

Figure S2. Size exclusion chromatography of BAK1-CD. BAK1-CD (3 mg/mL) was injected onto a Superdex 75 10/300 GL column. The retention volume is 13 mL. The retention volumes for the molecular weight standards are shown above.

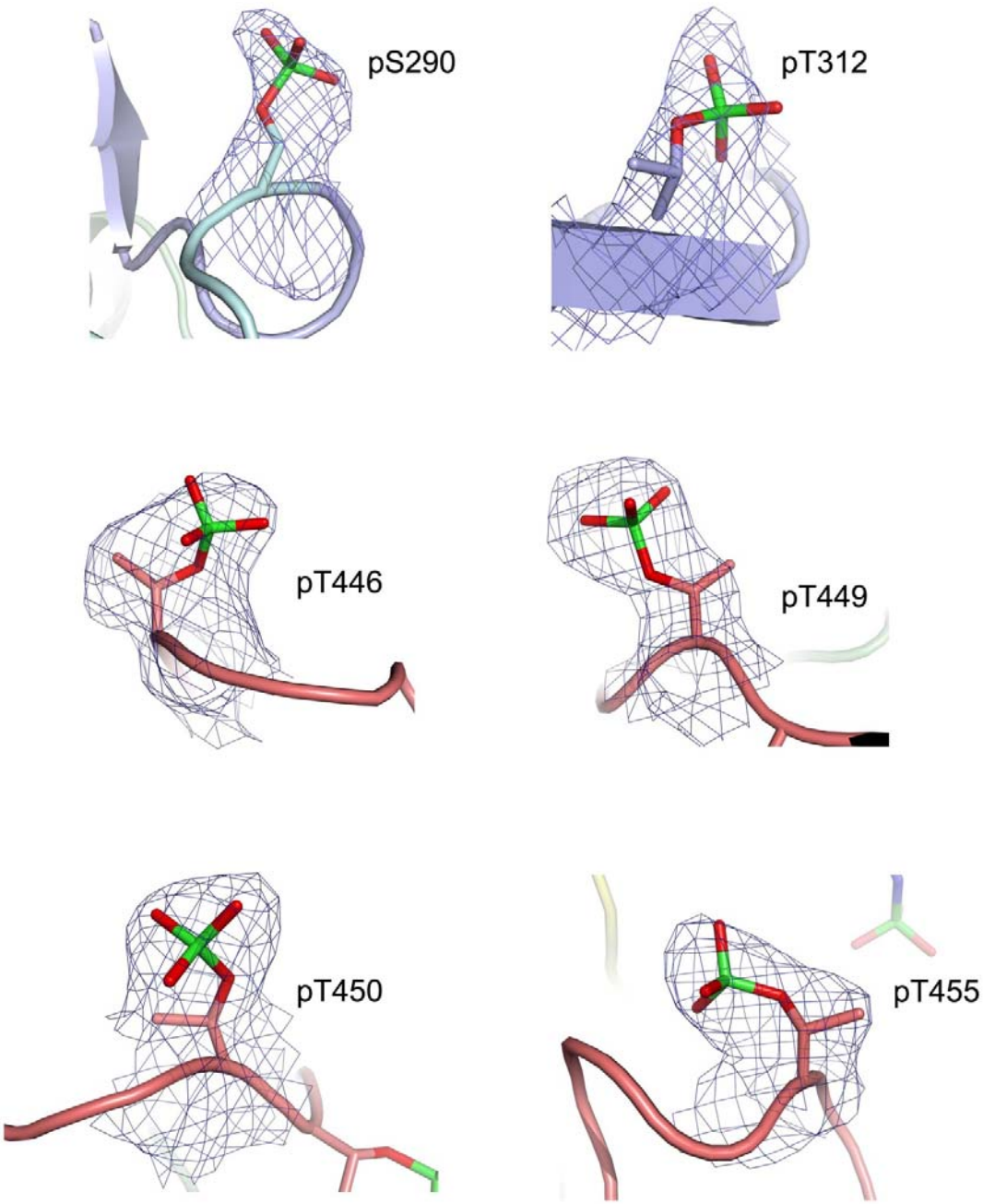

Figure S3. Electron density of the phosphorylated residues of BAK1-CD. pS290, pT312, pT446, pT449, pT450, and pT455, which are located at the activation loop, are shown as stick representations and covered by electron density clouds (*2Fo-Fc* map at 1.2σ).

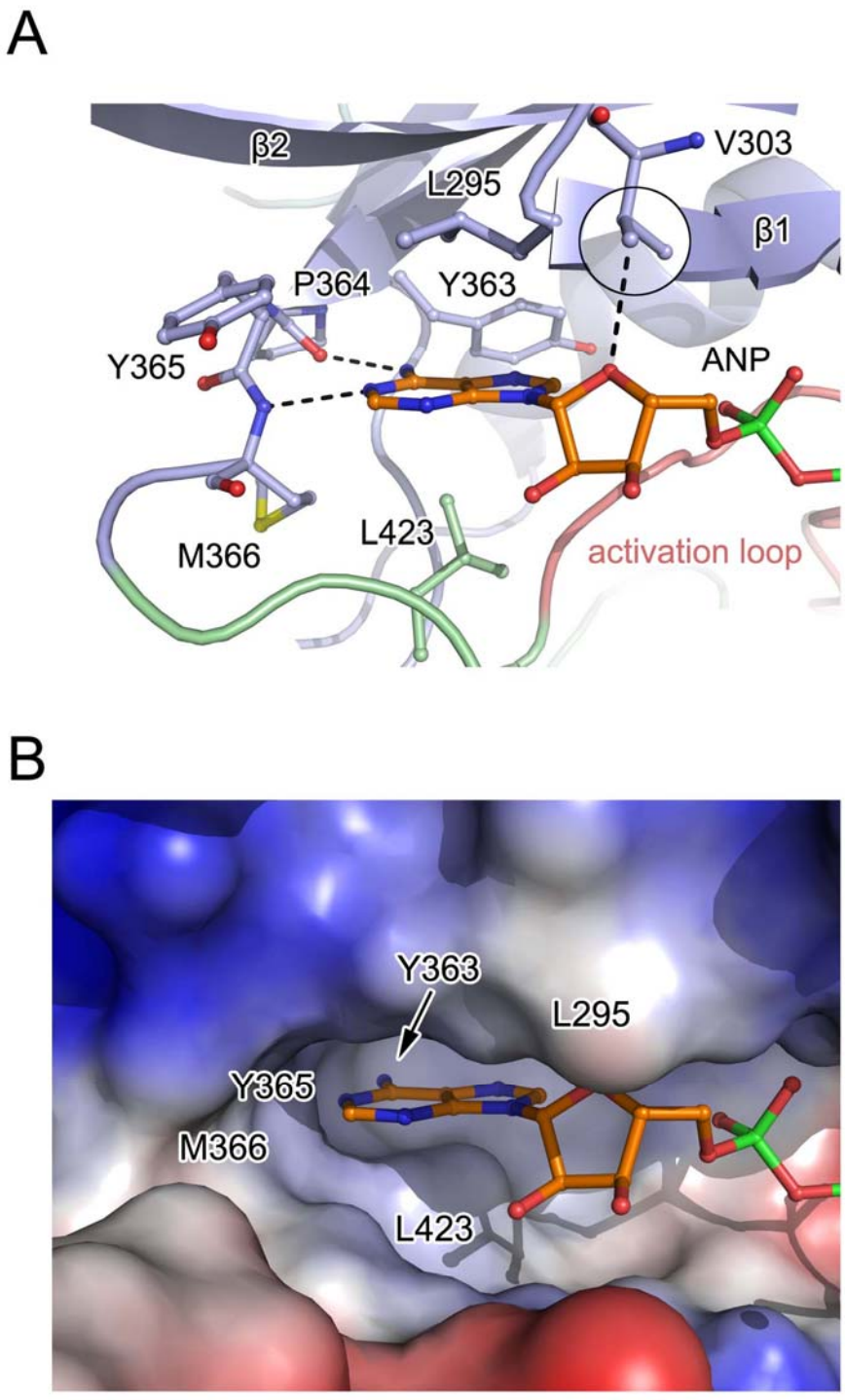

Figure S4. ATP-binding pocket of BAK1-CD. An adenosine-binding pocket is shown as a cartoon **(A)** and as an electron potential surface **(B)**. The BAK1-CD

molecule is shown as a cartoon with the same color scheme as that in Figure 1. The key residues for the adenosine-binding pocket are represented as colored sticks. The dashed lines represent hydrogen bonds.

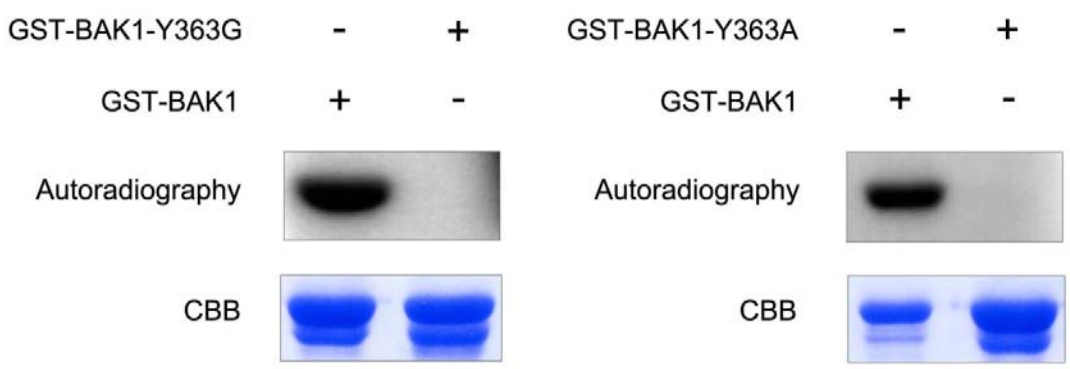

Figure S5. Substitutions on Y363 impair the autophosphorylation of BAK1-CD. An *in vitro* kinase assay was performed by incubating GST-BAK1 with GST-BAK1-Y363G and GST-BAK1-Y363A. The proteins were separated using sodium dodecyl sulfate polyacrylamide gel electrophoresis (SDS-PAGE) and analyzed via autoradiography (upper image). Protein loading control was determined via Coomassie blue staining (lower image).

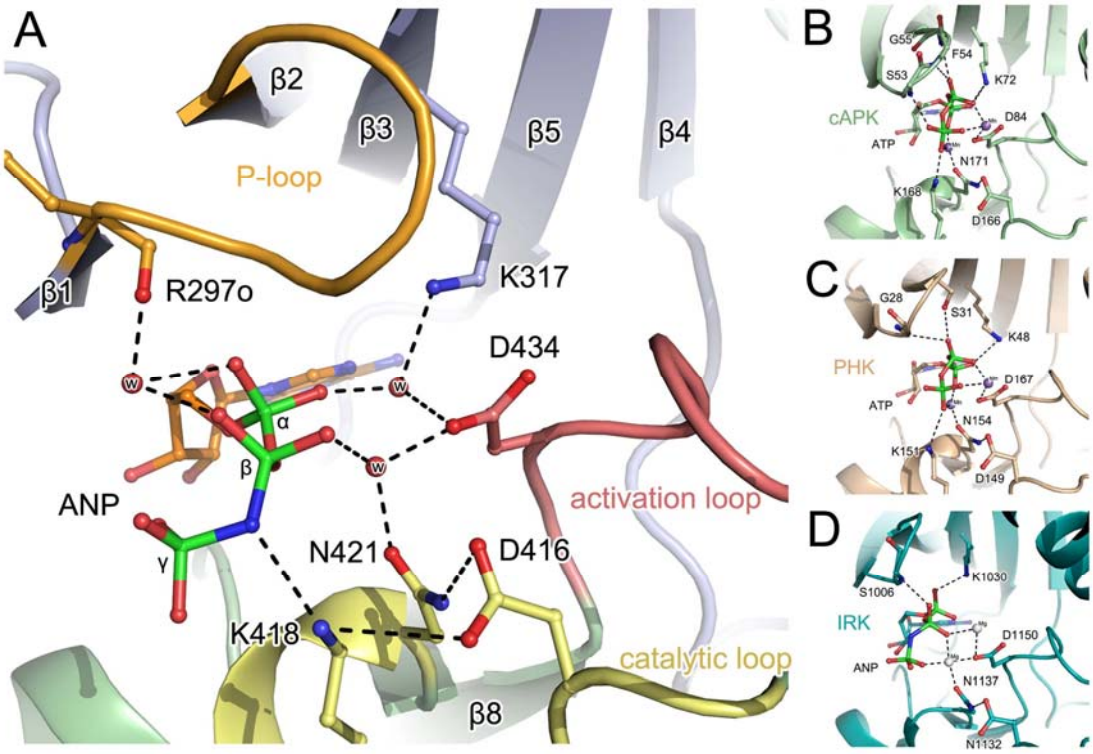

Figure S6. Comparison of the catalytic machinery involved in ATP hydrolysis. (A) Structure of the BAK1 kinase catalytic machinery. The red spheres labeled with "w" represent the water molecules involved in ATP binding. The dashed lines denote hydrogen bonding interactions. **(B–D)** Comparison of catalytic machineries in **(B)** cAPK (PDB: 1ATP), **(C)** PHK (PDB code: 2PHK), and **(D)** IRK (PDB code: 1IR3). Note the similar coordination by switch I in each case. All structures are aligned with BAK1-CD-ANP and shown with the same orientation.

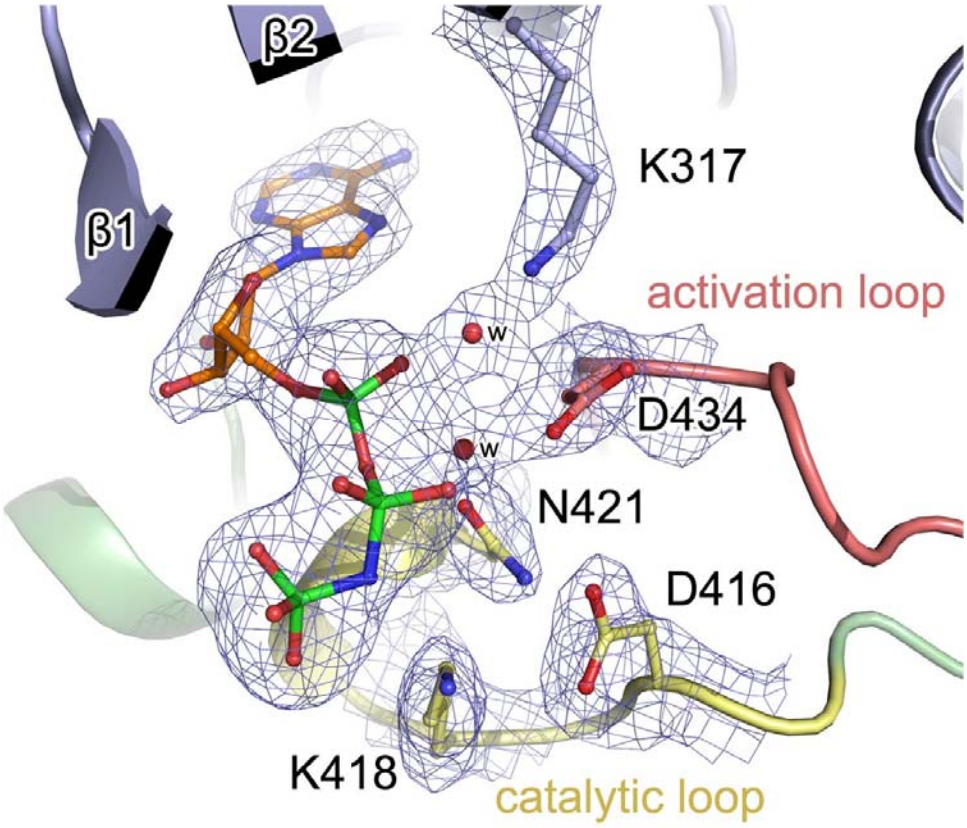

Figure S7. Electron density of the active sites of BAK1-CD. The red spheres labeled with "w" represent the water molecules involved in AMP–PNP binding. The bound AMP–PNP, catalytic residues, and associated water molecules are covered by *2Fo-Fc* map at 1.1σ.

Figure S8(A)

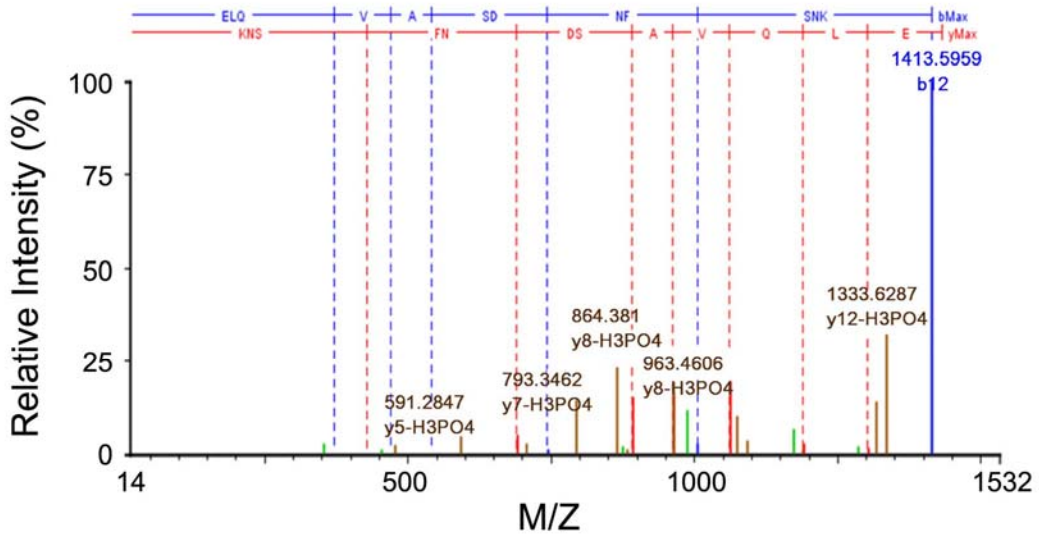

Figure S8(B)

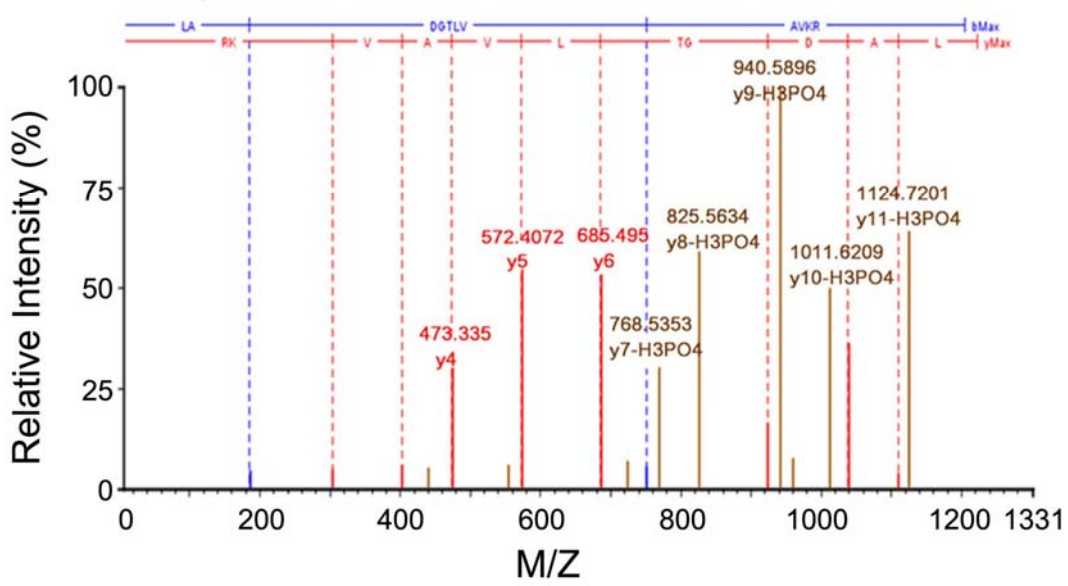

Figure S8(C)

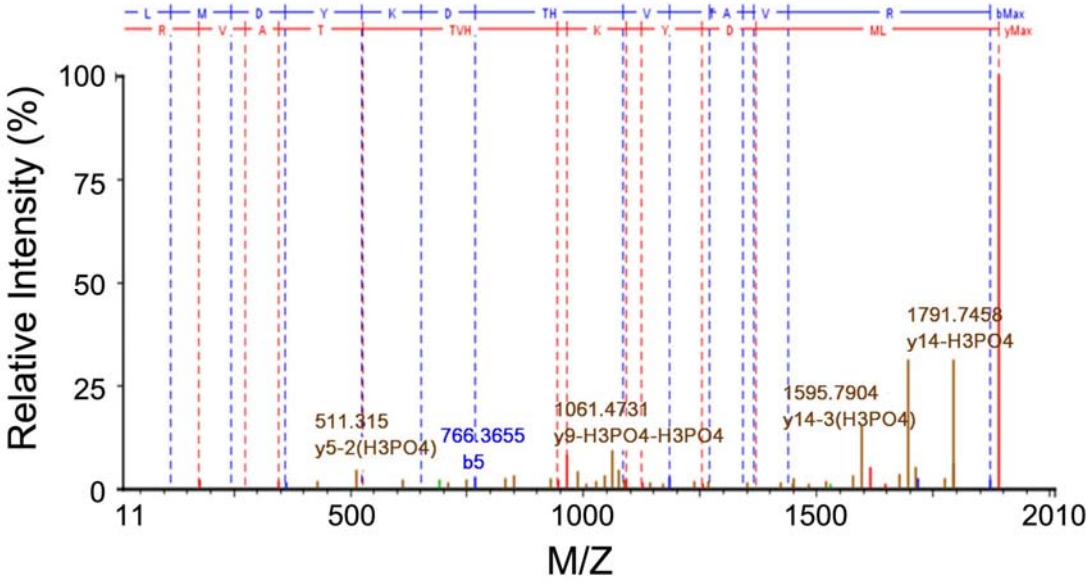

Figure S8(D)

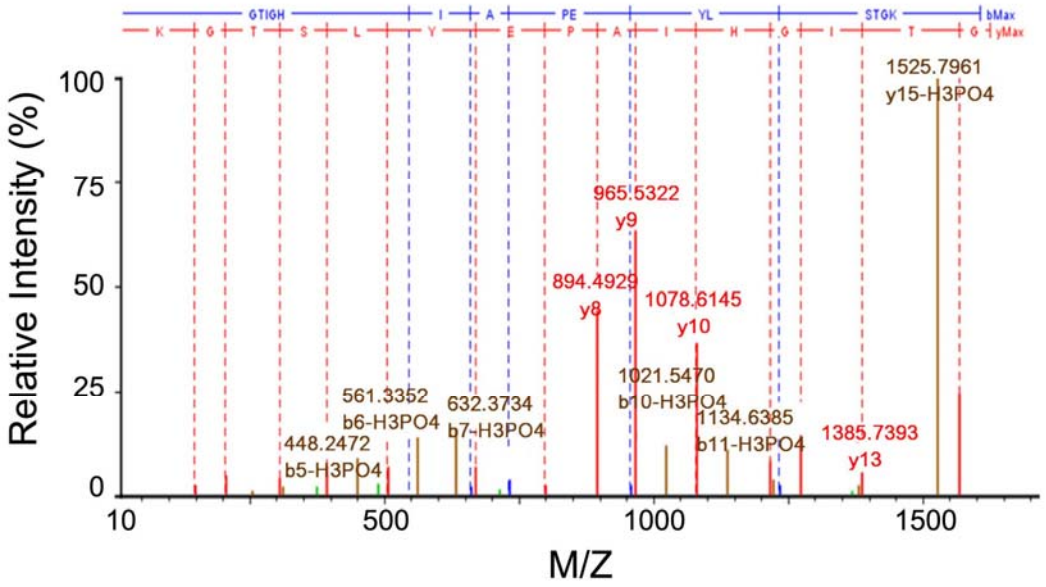

Figure S8. MS/MS spectra of phosphorylated peptides from BAK1-CD tryptic digestion. The neutral loss of the phosphate group from the peptide precursor and particular fragment ions is strong evidence for the assignment of

modification sites. Each spectrum is manually inspected to confirm the assignment. The peptide sequences for the individual spectrum are as follows: (A) ELQVASDNF**pS**NK; (B) LADG**pT**LVAVK; (C) LMDYKD**pT**HV**pTpT**AVR; and (D) G**pT**IGHIAPEYLSTGK.

Figure S9(A)

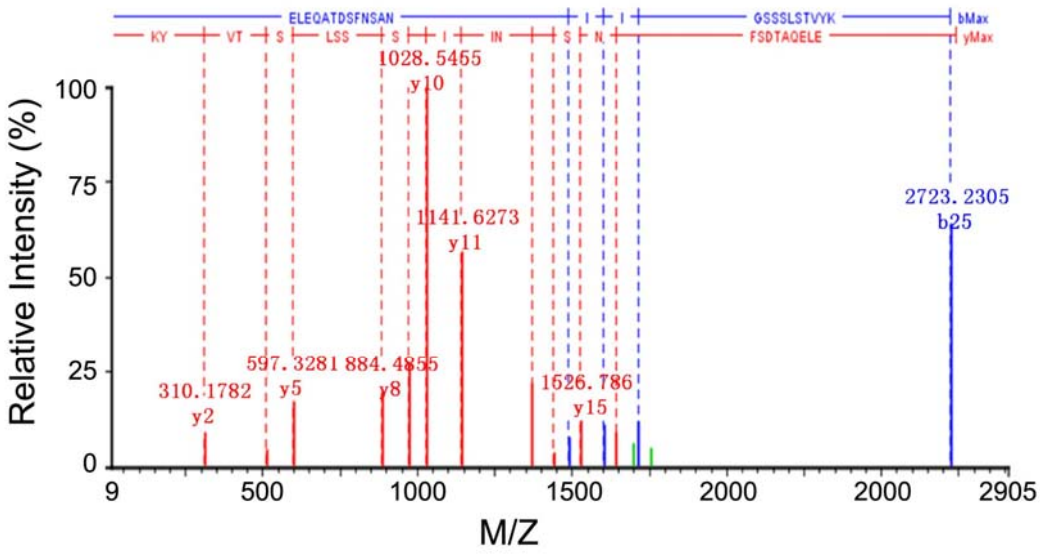
ELEQATDSFNSAN
GSSSLSTVYK
bMax
KY
VT
S
LSS
S
I
IN
S
N
FSDTAQELE
yMax
1028.5455
y10
1141.6273
y11
2723.2305
b25
597.3281
y5
884.4855
y8
310.1782
y2
1526.786
y15
Relative Intensity (%)
100
75
50
25
0
9
500
1000
1500
2000
2000
2905
M/Z

Figure S9(B)

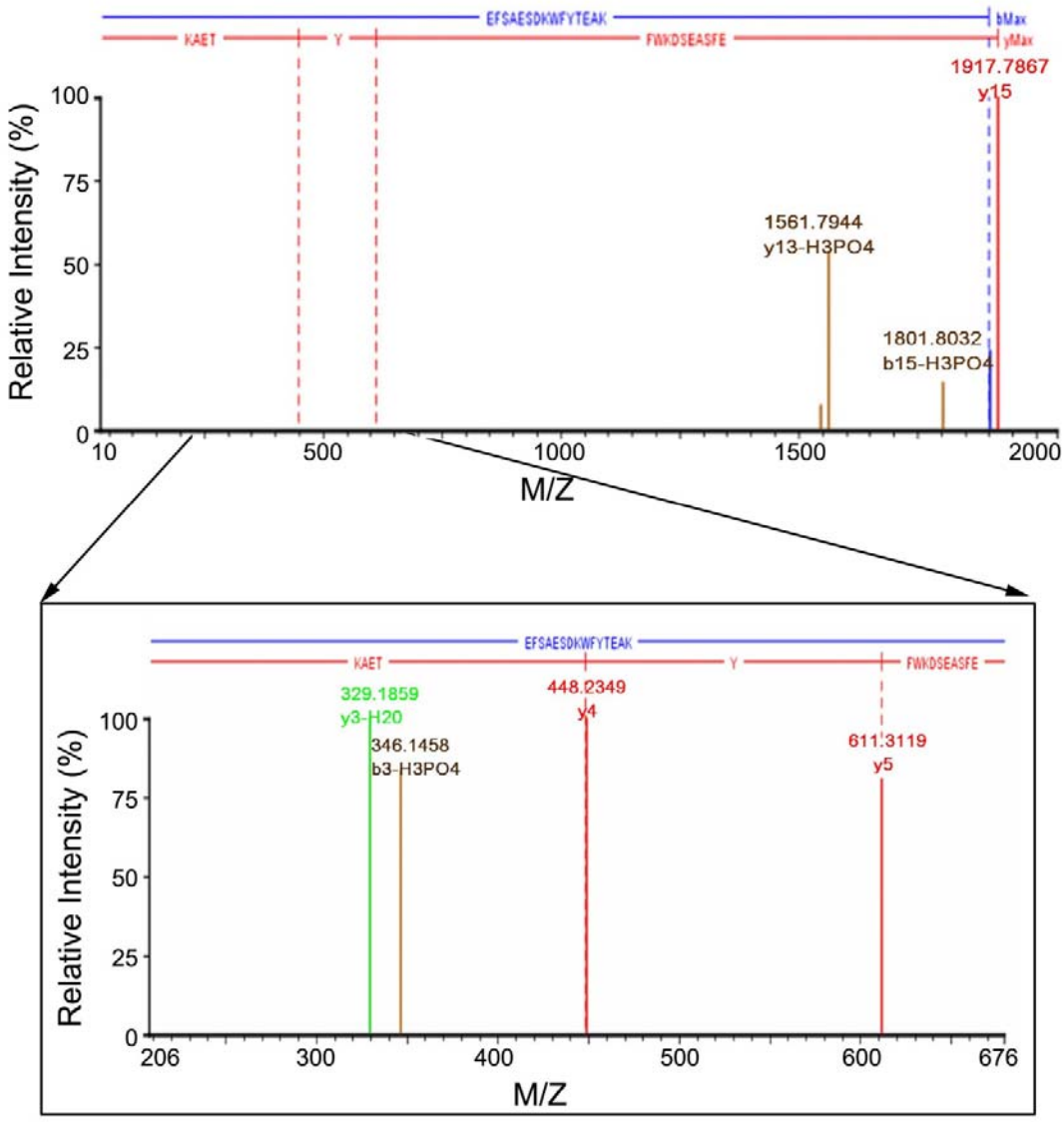
EFSAESDKWFYTEAK
bMax
KAET
Y
FWKDSEASFE
yMax
1917.7867
y15
1561.7944
y13-H3PO4
1801.8032
b15-H3PO4
Relative Intensity (%)
M/Z
329.1859
y3-H20
346.1458
b3-H3PO4
448.2349
y4
611.3119
y5

Figure S9(C)

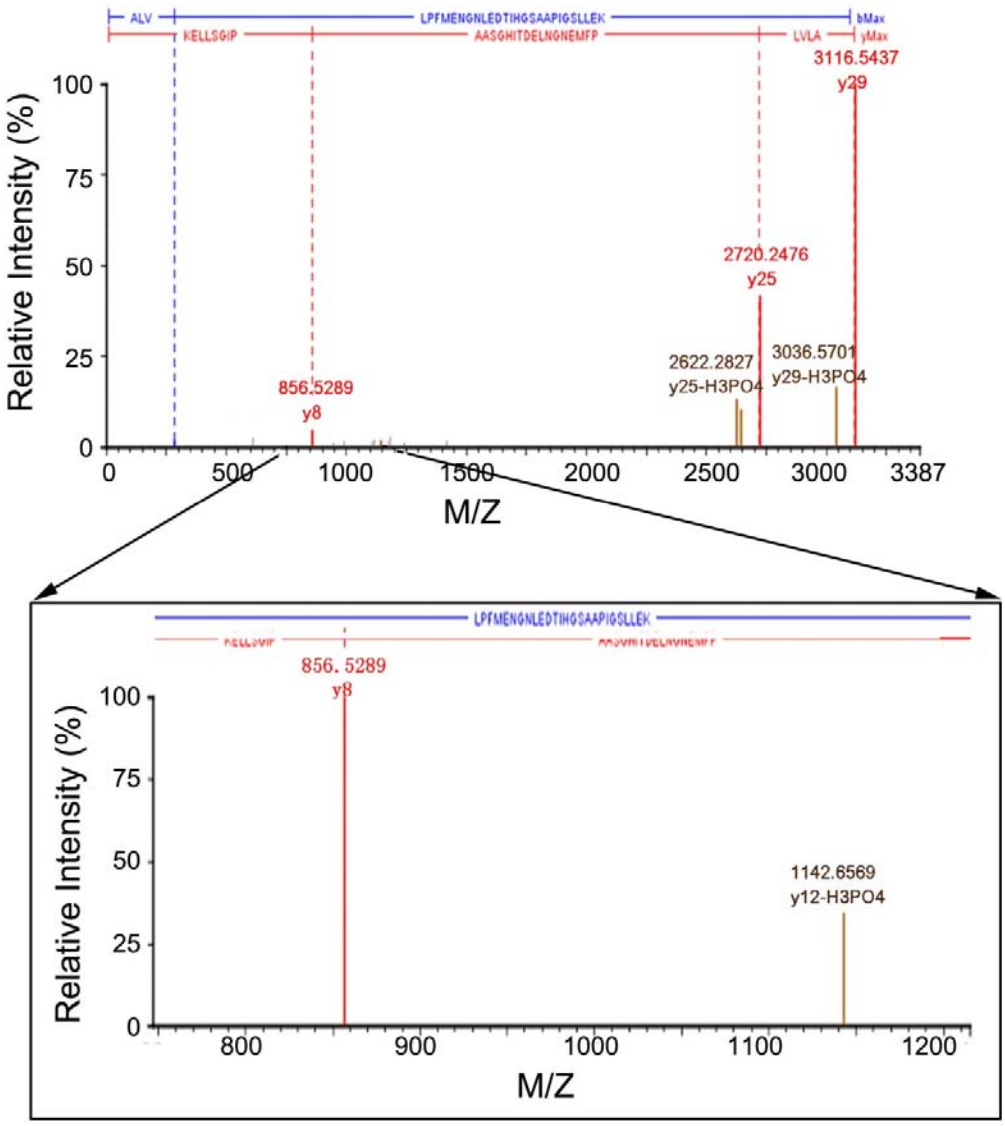
ALV
LPFMENGNLEDTIHGSAAPIGSLLEK
bMax
KELLSGIP
AASGHITDELNGNEMFP
LVLA
yMax
3116.5437
y29
2720.2476
y25
2622.2827
y25-H3PO4
3036.5701
y29-H3PO4
856.5289
y8
Relative Intensity (%)
M/Z
1142.6569
y12-H3PO4

Figure S9(D)

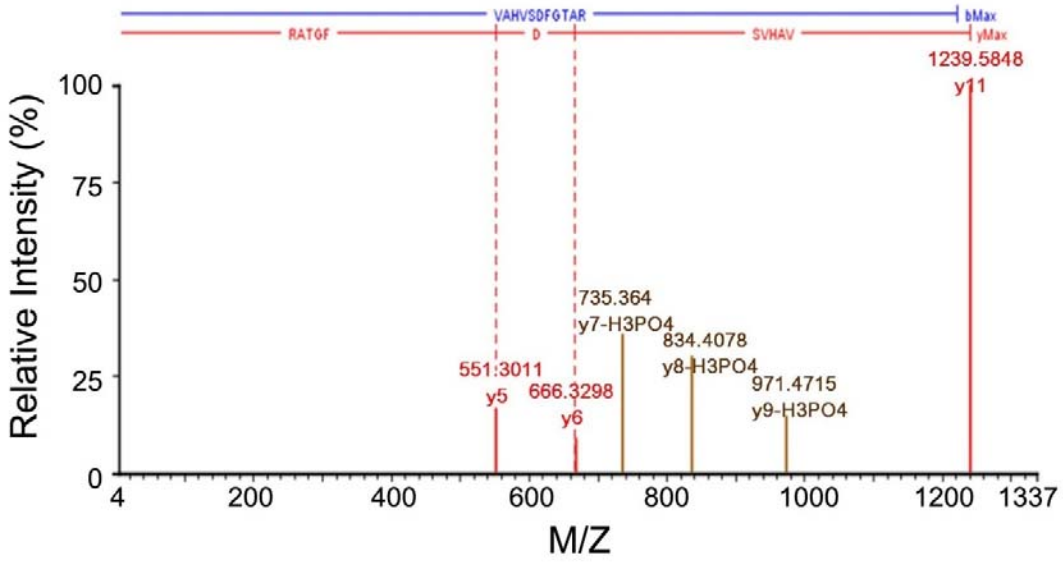
VAHVSDFGTAR
bMax
RATGF
D
SVHAV
yMax
1239.5848
y11
Relative Intensity (%)
100
75
50
25
0
735.364
y7-H3PO4
834.4078
y8-H3PO4
971.4715
y9-H3PO4
551.3011
y5
666.3298
y6
4
200
400
600
800
1000
1200
1337
M/Z

Figure S9(E)

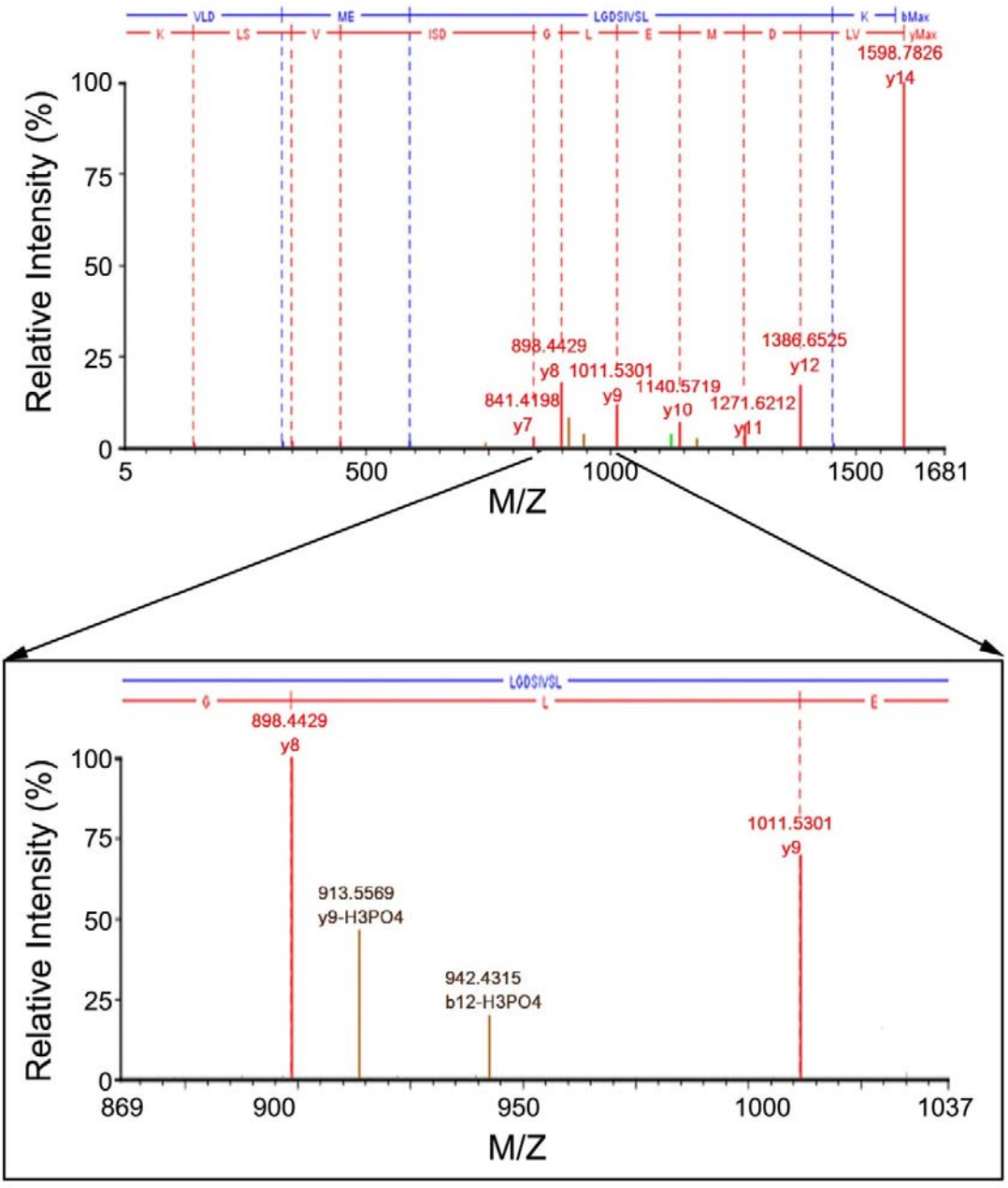

Figure S9. MS/MS spectra of the phosphopeptides from FLS2-CD upon BAK1-CD treatment. The neutral loss of the phosphate group from the peptide precursor and particular fragment ions is strong evidence for the assignment of modification sites. The peptide sequences for the individual spectrum are as

follows: (A) ELEQATD**pS**FNSANIIGSSSLSTVYK; (B) EF**pS**AESDKWFYTEAK; (C) ALVLPFMENGNLEDTIHG**pS**AAPIGSLLEK; (D) VAHV**pS**DFGTAR; (E) VLDMELGD**pS**IVSLK.

Table S1 Identification of autophosphorylation sites on BAK1-CD via high-resolution MS.

Autophosphorylation site[a]	Peptide sequence[b]	Mass error for peptide identification[c]
S290	ELQVASDNF**pS**NK	1.1 ppm
T312	LADG**pT**LVAVK	3.8 ppm
T446, T449, T450	LMDYKD**pT**HV**pTpT**AVR	0.6 ppm
T455	G**pT**IGHIAPEYLSTGK	2.8 ppm

[a]Phosphate groups on these sites were all clearly seen in the crystal structure of BAK1-CD.

[b]Peptide sequences identified via MS/MS analysis of the tryptic digests.

[c]Deviation of the measured peptide mass from its theoretical value in parts per million (ppm)

Table S2A. Identification of phosphopeptides from FLS2-CD upon BAK1-CD treatment by using high-resolution mass spectrometry

Putative phosphorylation site[a]	Peptide sequence[b]	Mass error for peptide identification[c]
S869	ELEQATD**pS**FNSANIIGSSSLSTVYK[d]	2.6 ppm
S906	EF**pS**AESDKWFYTEAK	4.3 ppm
S961	ALVLPFMENGNLEDTIHG**pS**AAPIGSLLEK	1.2 ppm
S1014	VAHV**pS**DFGTAR	2.7 ppm
S1115	VLDMELGD**pS**IVSLK	3.8 ppm

[a]The phosphorylate sites were automatically assigned by software and verified afterwards by manually inspecting the MS/MS spectra. More details on our criteria for peptide identification and site annotation as well as MS/MS spectra of these phosphopeptides were provided in Supplemental Materials.

[b]Peptide sequences identified by MS analysis of the tryptic digests. “pS” is the phosphorylated Ser.

[c]Deviation of the measured peptide mass from its theoretical value in the unit of parts per million (ppm)

[d]The inadequate MS/MS spectrum doesn’t fully support the automatically assigned phosphorylation site, suggesting the modification site cannot be exclusively determined, although the number of phosphorylation carried by the peptide can be established.

Table S2B. Relative changes of transphosphorylation of FLS2-CD by BAK1-CD mutants compared to the wide-type

BAK1-CD mutants	$S869^{FLS2}$	$S906^{FLS2}$	$S961^{FLS2}$	$S1014^{FLS2}$	$S1115^{FLS2}$
$D416A^{BAK1}$	ND [a]	ND	ND	ND	ND
$T446A^{BAK1}$	5.6%± 2.9% [b]	ND	9.8%± 2.7%	31.4%±0%	20.0%± 0%
$T449A^{BAK1}$	47.0%± 5.9%	30.0%± 9.9%	37.5%± 7.6%	58.9%± 17.6%	76.4%± 7.6%
$T450A^{BAK1}$	ND	ND	ND	ND	ND
$T455A^{BAK1}$	3.7%± 0.7%	ND	ND	ND	ND

[a] meaning no detection of the peptide MS signal

[b] Relative percentage of the MS response of a specific phosphopeptide from FLS2-CD incubated with the BAK1 mutant *vs* the wide-type. Standard deviations represent variation of the relative quantitation from experimental duplicates.

Table S3. Reproducibility of the quantitative analysis results of site-specific phosphorylation in wild-type BAK1-CD using our label-free MS-based approach

	S290 level	T312 level	T446-T450 level	T455 level
MS signal of phosphopeptides[a]	2.32±0.22[b]	0.15±0.05	4.97±0.47	3.63±0.35

[a]MS signal refers to the XIC response of each phosphopeptide modified on a specific site or multiple sites (triphosphorylation for the peptide covering T446-T450) normalized by the MS intensity of the internal standard (i.e., the beta-casein phosphopeptide).

[b]Standard deviation represents the variation in five experimental replicates, starting from protein digestion to MS analysis.

Table S4. Relative changes in the site-specific phosphorylation levels of the BAK1-CD mutants compared with those of the wild-type.

Subgroup	Relevant mutants	S290 relative[a]	T312 relative	T446-T450 relative	T455 relative
Catalytic base	D416A	ND[b]	ND	ND[c]	ND
	D421A	ND	ND	ND	ND
Subgroup I	R415G	2.3%±0.5%	ND	ND	2.2%±0.2%
	R415C	14.3%±1.6%	ND	51.9%±2.0%[d]	14.6%±2.7%
	K439A	24.3%±0.3%	11.4%±0,4%	ND	18.2%±0.2%
	*T450A	ND	ND	ND	ND
	R453G	79.7%±7.7%	100%	Pos	3.5%±2.4%
Subgroup II	*T455A	4.0%±1.5%	15.6%±4.4%	0.9%±0.5%	ND
	H458A	ND	ND	ND	ND
Subgroup III	*T446A	11.6%±0.6%	ND	ND	16.0%±2.3%
	H447A	25.41%±1.6%	72.4%±0.4%	Pos[e]	56.7%±1.2%
	*T449A	77.5%±0.7%	22.6%±0.1%	ND	58.7%±0.4%

[a]Relative percentage of the MS response of a specific phosphopeptide from the mutant vs the wild-type. The standard deviations represent the variation in the relative quantitation data from experimental duplicates.

[b]The peptide MS signal was not detected

[c]In this column, phosphorylation was detected on any of the three Thr residues in the peptide sequence. ND indicates not only triphosphorylation, but also mono- or di-phosphorylation, which were not detected via MS analysis.

[d]Diphosphorylation was detected on the peptide of this mutant, with a relative phosphorylation at 825%±48% vs the wild-type. Monophosphorylation was also detected on the peptide (site assignment is not conclusive), although it was not found in the wild-type.

[e]Point mutation changed the peptide sequence in this case; hence, its MS response cannot be compared with that of the wild-type for relative quantitation. “Pos” indicates that the mutant peptide was triphosphorylated based on its MS signal.

*Autophosphorylation sites in BAK1-CD

Table S5. Data collection and refinement statistics.

Parameters	BAK1-CD-apo	BAK1-CD-ANP
Data collection statistics		
Cell parameters		
a (Å)	70.3	70.1
b (Å)	75.6	74.7
c (Å)	71.9	71.2
α, β, γ (°)	90.0, 93.1, 90.0	90.0, 93.7, 90.0
Space group	C2	C2
Wavelength used (Å)	1.0000	1.0000
Resolution (Å)	50.00 (2.78)[c]–2.60	50.00 (2.26)–2.20
Number of all reflections	218,698 (10,900)	147,845 (8,537)
Number of unique reflections	28,872 (1,454)	19,638 (1,355)
Completeness (%)	100.0 (100.0)	97.5 (94.7)
Average I/σ (I)	6.2 (3.4)	13.4 (3.2)
R_{merge}[a] (%)	14.4 (44.8)	6.0 (59.6)
Refinement statistics		
Number of reflections used [$\sigma(F) > 0$]	26,050	19,314
R_{work}[b] (%)	24.1	23.6
R_{free}[b] (%)	28.9	28.4
r.m.s.d. bond distance (Å)	0.011	0.008
r.m.s.d. bond angle (º)	1.735	1.354

Average B-value (Å^2)	54.7	45.1
Number of protein atoms	10,552	2,359
Number of ligand atoms	0	31
Number of solvent atoms	383	170
Ramachandran plot		
Res. in favored regions (%)	92.8	93.8
Res. in generously allowed regions (%)	5.9	5.5
Res. in disallowed regions (%)	1.2	0

[a]R_{merge} = $\Sigma_h\Sigma_I$ | I_{ih}–<I_h> |/$\Sigma_h\Sigma_I$ <I_h>, where <I_h> is the mean of the observations I_{ih} of reflection h.

[b]R_{work} = Σ(||F_p(obs)|–|F_p(calc)||)/ $\Sigma|F_p(obs)|$; R_{free} is an R factor for a selected subset (5%) of the reflections that was not included in prior refinement calculations.

[c]Numbers in parentheses are the corresponding values for the highest resolution shell.

References for the supplementary materials

1 Otwinowski Z, Minor W. Processing of X-ray diffraction data collected in oscillation mode. In: Carter Jr. CW, Sweet RM. eds. Macromolecular Crystallography, part A: Academic Press 1997:307-326.

2 Matthews BW. Solvent content of protein crystals. J Mol Biol 1968; 33:491-497.

3 McCoy A, Grosse-Kunstleve R, Adams P, Winn M, Storoni L, Read R. Phaser crystallographic software. J Appl Cryst 2007; 40:658-674.

4 Wang Z, Liu J, Sudom A et al. Crystal structures of IRAK-4 kinase in complex with inhibitors: a serine/threonine kinase with tyrosine as a gatekeeper. Structure 2006; 14:1835-1844.

5 Emsley P, Cowtan K. Coot: model-building tools for molecular graphics. Acta Crystallogr D Biol Crystallogr 2004; 60:2126-2132.

6 Adams PD, Grosse-Kunstleve RW, Hung LW et al. PHENIX: building new software for automated crystallographic structure determination. Acta Crystallogr D Biol Crystallogr 2002; 58:1948-1954.

7 Laskowski R, MacArthur M, Moss D, Thornton J. PROCHECK: a program to check the stereochemical quality of protein structures. J Appl Cryst 1993; 26:283-291.

8 DeLano W. The PyMOL Molecular Graphics System 2002.

9 Wang X, Kota U, He K et al. Sequential transphosphorylation of the BRI1/BAK1 receptor kinase complex impacts early events in brassinosteroid signaling. Dev Cell 2008; 15:220-235.

10 Yun HS, Bae YH, Lee YJ et al. Analysis of phosphorylation of the BRI1/BAK1 complex in arabidopsis reveals amino acid residues critical for receptor formation and activation of BR signaling. Mol Cells 2009; 27:183-190.

11 Schwessinger B, Roux M, Kadota Y et al. Phosphorylation-dependent differential regulation of plant growth, cell death, and innate immunity by the regulatory receptor-like kinase BAK1. PLoS Genet 2011; 7:e1002046.